## Title

Molecular Profiling of Prostatic Acinar Morphogenesis Identifies PDCD4 and KLF6 as Tissue Architecture–Specific Prognostic Markers in Prostate Cancer



## Journal

American Journal Of Pathology, 182(2)

## ISSN

0002-9440

## Authors

Li, Chi-Rong
Su, Jimmy J-M
Wang, Wei-Yu
et al.

## Publication Date

2013-02-01

## DOI

10.1016/j.ajpath.2012.10.024

Peer reviewed

The American Journal of Pathology, Vol. 182, No. 2, February 2013

The American Journal of
PATHOLOGY
ajp.amjpathol.org

BIOMARKERS, GENOMICS, PROTEOMICS, AND GENE REGULATION

# Molecular Profiling of Prostatic Acinar Morphogenesis Identifies *PDCD4* and *KLF6* as Tissue Architecture—Specific Prognostic Markers in Prostate Cancer

Chi-Rong Li,*† Jimmy J.-M. Su,* Wei-Yu Wang,* Michael T.-L. Lee,‡ Ting-Yun Wang,* Kuan-Ying Jiang,* Chein-Feng Li,§ Jong-Ming Hsu,¶ Chi-Kuan Chen,¶ Marcelo Chen,¶ Shih-Sheng Jiang,* Valerie M. Weaver,‖ and Kelvin K.-C. Tsai**

*From the National Institute of Cancer Research and the Translational Center for Glandular Malignancies,* the National Health Research Institutes, Tainan, Taiwan; the Department of Medical Education and the School of Nursing,† Chung Shan Medical University and Hospital, Taichung, Taiwan; the Department of Information Engineering,‡ Kun Shan University, Tainan, Taiwan; the Department of Pathology,§ Chimei Foundational Medical Center, Tainan, Taiwan; the Department of Urology and Pathology,¶ Mackay Memorial Hospital, Taipei, Taiwan; the Departments of Surgery, Anatomy and Bioengineering and Therapeutic Sciences,‖ the Center for Bioengineering and Tissue Regeneration, Eli and Edythe Broad Center of Regeneration Medicine and Stem Cell Research and Helen Diller Family Comprehensive Cancer Center, University of California, San Francisco, San Francisco, California; and the Graduate Institute of Clinical Medicine, the School of Medicine,** Taipei Medical University, Taipei, Taiwan*

Accepted for publication October 31, 2012.

Address correspondence to Kelvin K.-C. Tsai, M.D., Ph.D., National Institute of Cancer Research, National Health Research Institutes, Sheng-Li Road, 1F, No. 367, Tainan 70456, Taiwan. E-mail: tsaik@nhri.org.tw.

Histopathological classification of human prostate cancer (PCA) relies on the morphological assessment of tissue specimens but has limited prognostic value. To address this deficiency, we performed comparative transcriptome analysis of human prostatic acini generated in a three-dimensional basement membrane that recapitulates the differentiated morphological characteristics and gene expression profile of a human prostate glandular epithelial tissue. We then applied an acinar morphogenesis—specific gene profile to two independent cohorts of patients with PCA (total $n = 79$) and found that those with tumors expressing this profile, which we designated acini-like tumors, had a significantly lower risk of postoperative relapse compared with those tumors with a lower correlation (hazard ratio, 0.078; log-rank test $P = 0.009$). Multivariate analyses showed superior prognostic prediction performance using this classification system compared with clinical criteria and Gleason scores. We prioritized the genes in this profile and identified programmed cell death protein 4 (*PDCD4*) and Kruppel-like factor 6 (*KLF6*) as critical regulators and surrogate markers of prostatic tissue architectures, which form a gene signature that robustly predicts clinical prognosis with a remarkable accuracy in several large series of PCA tumors (total $n = 161$; concordance index, 0.913 to 0.951). Thus, by exploiting the genomic program associated with prostate glandular differentiation, we identified acini-like PCA and related molecular markers that significantly enhance prognostic prediction of human PCA. *(Am J Pathol 2013, 182: 363—374; http://dx.doi.org/10.1016/j.ajpath.2012.10.024)*

Prostate cancer (PCA) is a leading cause of cancer-related death in men. For early-stage localized prostate cancer, radical prostatectomy offers the best opportunity to eradicate the disease. However, approximately 15% to 30% of patients with localized disease at diagnosis develop recurrence within 5 to 10 years, and most of these patients subsequently show poor therapeutic outcome.[1,2] Strategies to stratify the initially diagnosed disease into higher-risk patients with PCA would permit a more personalized targeted treatment strategy that could prevent recurrence. Moreover, a deeper understanding of the pathomolecular mechanisms underlying disease recurrence would help to identify new therapeutic targets.

Such as most glandular cancers, the malignant transformation of prostatic epithelium involves a gradual loss of cell adhesion and normal glandular architecture.[3—7] Loss of the ability to form tissue architectures by prostate epithelial

Supported by the National Health Research Institutes Intramural Research Program grant (CA-100-PP-19 to K.K.-C.T.), National Science Council (NSC) grant (96-2321-B-038-004 to K.K.-C.T.), National Core Facility Program for Biotechnology Grants of NSC (NSC 100-2319-B-400-001), an NSC grant (99-2218-E-168-004 to M.T.-L.L.), Department of Health grant (DOH100-TD-C-111-004 to K.K.-C.T.), and National Cancer Institute grants (P50 CA 58207 and R01 CA140663-01A2 to V.M.W.).

C.-R.L. and J.J.-M.S. contributed equally to this work.


http://dx.doi.org/10.1016/j.ajpath.2012.10.024

cells has been functionally linked to increased tumorigenicity.[5] Because human PCA frequently displays considerable intratumoral heterogeneity in glandular differentiation, this spectrum of tissue morphological characteristics is widely used to classify PCA pathological features according to metrics, such as the Gleason grading system.[7] Large-scale clinical studies have established the degree of glandular differentiation as a reasonable determinant to assess the clinical behavior of PCA. Specifically, poorly differentiated, high—Gleason grade tumors are typically associated with a higher probability of tumor recurrence, and patients with these tumors often show poorer prognosis.[8,9] Nevertheless, this morphological characteristic—based classification system is only modestly prognostic and does not allow for risk stratification of PCA with similar histopathological characteristics.

Tumor classification based solely on tissue architecture has failed to provide functional or mechanistic insights into tumor variability. Accordingly, there is a critical need for molecularly based diagnostic assays that can increase the accuracy of disease prognosis and clinical outcome in PCA. Recently, high-throughput genomic profiling techniques have been applied to molecularly characterize several human malignancies, including PCA, with encouraging success.[10–15] The profound prognostic utility of these genomic markers underlines the intrinsic molecular characteristic of tumors as a crucial determinant to their clinical behavior and has laid the framework for personalized medicine. Genomic tools have also been used to molecularly define tumor phenotypes or subtypes. For example, transcript profiling of human PCA has supported the existence of distinct tumor subclasses that are associated with distinct tumor grades and stage.[16] Furthermore, gene expression patterns that correlate with Gleason score and distinguish low- from high-grade PCA have been described.[6,17] These molecular patterns of PCA are instructive, and they can help to characterize tumor characteristics. However, the mechanisms underlying the genesis of these molecular variations in human PCA remain to be further explored.

Knowledge-based approaches offer an opportunity to identify more rational markers or classification systems that benefit clinical decision making and therapeutic advancement. Such approaches have been used to establish the prognostic roles of gene profiles associated with tumor progenitor cells, stromal activation, or tissue differentiation in several types of solid tumors.[18–21] Whether a similar approach could be applied to improve the prognostic prediction of PCA has yet to be determined. In this study, we exploited the experimental merits of a physiologically relevant model of tissue organization, thereby identifying a gene expression program that associates with prostate epithelial acinar morphogenesis. We constructed a gene signature that identifies a subset of more differentiated acini-like human PCAs with a favorable outcome. Relative to clinical criteria and Gleason score, this constructed, biologically informed molecular classification scheme displayed a more robust and accurate ability to predict the prognosis of human PCA. Uniquely, this signature consists of gene markers whose gene expression pattern depends on tissue architecture. The strength of this signature was validated as having strong prognostic value using several target genes as surrogate markers of tissue differentiation. Thus, to our knowledge, our results provide the first example of a biologically tractable and clinically instructive molecular signature for PCA that is based on criteria informed by tissue morphological characteristics.

## Materials and Methods

### Cell Culture and Staining

Primary human prostate epithelial cells (PrECs; Clonetics Cell Systems; Lonza, Walkersville, MD) were propagated on tissue culture plastics in chemically defined medium, according to the manufacturer's instructions. RWPE-1 cells (ATCC, Manassas, VA) were maintained in keratinocyte—serum-free medium (Invitrogen, Carlsbad, CA) supplemented with bovine pituitary extract, 10 ng/mL epidermal growth factor, and 0.5% penicillin-streptomycin (Invitrogen).[22] LNCaP, DU-145, and PC-3 cells (ATCC) were maintained in RPMI 1640 medium (for LNCaP cells) or Dulbecco's modified Eagle's medium (for DU-145 and PC-3 cells; Invitrogen) supplemented with 10% fetal bovine serum and 0.5% penicillin-streptomycin. The cells were embedded and grown within a thick layer of three-dimensional (3D) reconstituted basement membrane (rBM) gel (Matrigel; BD Biosciences, San Jose, CA), as previously described.[23] Whole culture immunofluorescent staining was performed as previously described.[24] Confocal imaging was performed using a Nikon Digital Eclipse C1 confocal microscope system (Nikon, Tokyo, Japan). The antibodies used include rat anti-$\alpha$6 integrin (clone GoH3; Millipore) and mouse anti-GM130 (clone 35; BD Biosciences). Cell nuclei were counterstained with Hoechst 33342 or DAPI (Invitrogen).

### Gene Expression Profiling

Total RNA samples were extracted from cells that were embedded and cultivated within the 3D rBM gels for different lengths of time (36 to 48 hours or 7 to 8 days) using TRIzol (Invitrogen) and then purified using an RNeasy minikit and DNase treatment (Qiagen, Valencia, CA). Experiments were performed in triplicate. Whole-genome gene expression analysis was performed on an Affymetrix Human Genome U133A 2.0 Plus GeneChip platform, according to the manufacturer's protocol (Affymetrix, Santa Clara, CA). The hybridization intensity data were processed using the GeneChip Operating software (Affymetrix), and the genes were filtered based on the Affymetrix P/A/M flags to retain those that were present in all three of the samples in at least one of the experimental conditions. A false-discovery

rate of <0.025 was used to select differentially expressed genes within a comparison group. The gene expression data have been deposited in the National Center for Biotechnology Information's Gene Expression Omnibus (*http://www.ncbi.nlm.nih.gov/geo*; accession number GSE30304).

### Quantitative Real-Time RT-PCR Analysis

Total RNA (1.0 μg) extracted from the 3D culture was used as a template for cDNA synthesis using Moloney Murine Leukemia Virus Reverse Transcriptase (Promega, Madison, WI). cDNA (100 ng) was used as a template for PCR amplification using the LightCycler FastStart DNA MASTER$^{PLUS}$ SYBR Green I Kit, and quantitative real-time RT-PCR analysis was performed on the amplified RNA using the LightCycler FastStart DNA MASTER-PLUS SYBR Green I Kit (Roche Diagnostics GmbH, Mannheim, Germany). Oligonucleotide primers were designed using Primer Bank (*http://pga.mgh.harvard.edu/primerbank/index.html*, last accessed June 10, 2012). The sequences are available on request.

### Hierarchical and Functional Gene Clustering

We median centered the genes identified from the gene expression profiling experiments and performed average linkage clustering using Cluster software version 2.11 and TreeView software version 1.60 (Eisen Lab, University of California, Berkeley). For functional clustering, the selected genes were uploaded to DAVID (*http://david.abcc.ncifcrf.gov*, last accessed March 28, 2012) and a ranked list of functional annotations was executed and generated by the system. We surveyed the functional annotations according to the gene ontology biological process, with $P < 0.05$, and the top 10 functional annotations, along with their associated genes, were displayed in a diagram output using Cytoscape software (*http://www.cytoscape.org*, last accessed March 28, 2012). Ingenuity Pathway Analysis (Ingenuity Systems, Redwood City, CA) was used to search for the enriched biological networks and functions of the selected genes.

### Gene Expression Data Sets of Human PCA

The tumor transcriptome data of 50 patients with PCA who underwent radical prostatectomy at Brigham and Women's Hospital (BWH cohort; Boston, MA) and the associated clinical information were previously reported and were kindly provided by Massimo Loda (Dana-Farber Cancer Institute, Boston).[10] Gene expression profiles of PCA and associated clinical information from 29 patients who underwent radical prostatectomy at Stanford University (Stanford, CA), Karolinska Institute (Solna, Sweden), and Johns Hopkins University (Baltimore, MD) (the SU/KI/JHU cohort) were downloaded from Gene Expression Omnibus (*http://www.ncbi.nlm.nih.gov/geo*; accession number GSE3933).[16]

### Measurement of Similarity between Gene Expression Profiles

To measure the degree of resemblance between the gene expression profiles of a clinical tumor specimen and a prostatic organoid, we mapped the selected probe sets from different microarray platforms to the same Entrez-gene IDs and then normalized and mean centered the probe hybridization intensity levels (for Affymetrix microarrays) or fluorescence ratios (for cDNA microarrays) of each of the selected probes across all tumors or the prostate architectures. For each tumor, we calculated the Pearson's correlation coefficient between the tumor and the organoid based on the expression profile of the selected gene probes.

### Construction of Prognostic Predictors

To identify, from the differentially expressed genes, a set of gene markers that optimally predicted risk of recurrence after radical prostatectomy in human PCA, we used a previously described supervised approach with modifications.[25] Briefly, for each gene, univariate Cox regression analysis was used to measure the correlation between the expression level of the gene (on a $\log_2$ scale) and the length of relapse-free survival of the patients with PCA in the BWH cohort. We constructed 1000 bootstrap samples of the patients in the cohort and performed Cox regression analysis on each of the samples. We then determined an estimated $P$ value and an estimated standardized Cox regression coefficient for each gene by calculating the median $P$ values and the median Cox coefficient of the 1000 bootstrap samples, respectively. To ensure the consistency of our model, we selected the genes whose expressional changes during prostatic cystic differentiation were associated with the expected positive (for genes with higher expression levels in cellular aggregates) or negative (for genes up-regulated in prostatic cysts) risk of relapse, as determined by the estimated standardized Cox regression coefficient. The selected genes were then rank ordered according to the estimated $P$ values, and multiple sets of genes were generated by repeatedly adding one more gene each time from the top of the descendingly ranked list, starting from the first three top-ranked genes. We then calculated a recurrence score (Equation 1) to measure the risk of relapse of a patient for a gene set:

$$\text{Recurrence score} = \sum_{i=3}^{k} b_i x_i \quad (1)$$

where $k$ is the number of probes in the probe set, $b_i$ is the standardized Cox regression coefficient for the $i$th probe, and $x_i$ is the $\log_2$ expression level for the $i$th probe.

For each selected probe set, the concordance index ($C$-index) was used to evaluate the predictive accuracy in survival analysis, where an index of 1.0 is perfect discrimination.[26]

### Gene Expression Manipulations

Sustained knockdown of programmed cell death protein 4 (*PDCD4*) or Kruppel-like factor 6 (*KLF6*) in RWPE-1 cells was achieved by retrovirus or lentivirus-mediated RNA interference (RNAi) using oligonucleotide sequences previously described[27] in the pSUPER.retro.neo system (OligoEngine, Seattle, WA) or validated short hairpin RNA oligonucleotides (MISSION shRNA lentiviruses). Amphotropic retrovirus was produced in Phoenix ampho cells (a gift from Garry Nolan, Stanford University), with packaging vectors pCgp and pVSV-G to boost viral titer.

### IHC Data

Formalin-fixed, paraffin-embedded (FFPE) tissues of human PCA from 61 patients who underwent radical prostatectomy at Chimei Foundational Medical Center (the CFMC cohort) or 50 patients at Mackay Memorial Hospital were acquired and used in conformity with Institutional Review Board–approved protocols (Table 1). The biochemical recurrence of PCA was defined as a prostate-specific antigen (PSA) level of at least 0.4 ng/mL or two consecutive PSA values of 0.2 ng/mL and increasing.[28] Tissue sections were deparaffinized, hydrated, and immersed in citrate buffer at pH 6.0 for epitope retrieval in a microwave. Endogenous peroxidase activity was quenched in 3% hydrogen peroxidase for 15 minutes, and slides were then incubated with 10% normal horse serum to block non-specific immunoreactivity. The antibody was subsequently applied and detected by using the DAKO EnVision kit (Dako, Carpinteria, CA). The antibodies used include anti-PDCD4 (1:4000, clone EPR3431), anti-KLF6 (1:50, polyclonal), and anti–ATP-binding cassette transporter 8 (ABCG1; 1:500, clone EP1366Y) (all from Epitomics, Burlingame, CA). All of the immunohistochemical (IHC) staining was evaluated by two expert pathologists (C.-F.Li and C.-K. Chen), and the staining patterns were quantified using the histological score (H-score).[29]

### Statistical Analysis

We used the statistical programming language R version 2.14.0 (*http://cran.r-project.org*) and SPSS software version 10.0 (SPSS, Chicago, IL), to conduct the statistical analysis of data. A two-tailed Student's *t*-test was used for simple significance testing, and two-tailed Pearson tests were used for correlation analysis. *C*-statistics analysis was conducted using the R survcomp package. A cutoff value that best discriminates between groups with respect to outcome was determined using the maximal Youden's index.[30] Survival curves were generated using the Kaplan-Meier method. The curves were plotted and compared using the log-rank test using GraphPad Prism software version 5.02 (GraphPad Software, La Jolla, CA). Statistical significance was considered if $P < 0.05$.

## Results

### Molecular and Functional Profiling of Prostatic Acinar Morphogenesis

The study of tissue-specific differentiation and tumorigenesis was greatly enhanced by the exploitation of 3D organotypic culture assays that use an rBM to recapitulate glandular-like tissues *ex vivo*.[5,31–34] Therefore, we applied this 3D rBM assay to gain molecular insight into prostatic epithelial cell morphogenesis and transformation. We noted that PrECs within 3D rBM grew rapidly within the first few days and formed small cellular aggregates (Figure 1A). After prolonged culture (7 to 8 days), most of the colonies assembled polarized, growth-arrested structures with an acinus-like architecture that was reminiscent of normal prostatic glands or differentiated low-grade PCA (Figure 1, A and B). Confocal imaging of spheroids stained for the polarity markers GM130 and α6(β4) integrin confirmed that these structures were composed of a single layer of cells with apico-basal polarity that surrounded a hollow central lumen (Figure 1A). Colonies of the immortalized prostate epithelial cell line, RWPE-1 cells,[22] embedded within rBM similarly yielded structurally differentiated acini. By contrast, malignant PCA cells, such as androgen-sensitive LNCaP cells, formed continuously growing, disorganized, and nonpolarized colonies that were morphologically indistinguishable from high-grade PCA (Figure 1, A and B).

After having recapitulated the acinar morphogenetic process of prostate epithelium, we next analyzed the gene

**Table 1** Patient Characteristics

| Clinical cohort | BWH group ($n = 50$) | SU/KI/JHU group ($n = 29$) | CFMC group ($n = 61$) | MMH group ($n = 50$) |
|---|---|---|---|---|
| Mean (SD) age (years) | 59.4 (6.8) | 59.0 (6.2) | 65.1 (5.6) | 67.4 (5.4) |
| Gleason score | | | | |
| 4-7 | 46 (92.0) | 22 (75.9) | 29 (47.5) | 20 (40.0) |
| 8-9 | 4 (8.0) | 7 (24.1) | 32 (52.5) | 30 (60.0) |
| Mean (SD) baseline PSA (ng/mL) | 8.3 (5.8) | NA | 18.8 (30.8) | 15.2 (3.6) |
| Tumor stage | | | | |
| I-II | 30 (60.0) | 19 (65.5) | 53 (86.9) | 42 (84.0) |
| ≥III | 20 (40.0) | 10 (34.5) | 8 (13.1) | 8 (16.0) |
| Recurrence | 9 (18.0) | 7 (24.1) | 11 (18.0) | 12 (24.0) |
| Medium time to recurrence (months) | 42.9 | 11.5 | 87.9 | 70.2 |

MMH, Mackay Memorial Hospital; NA, not available.

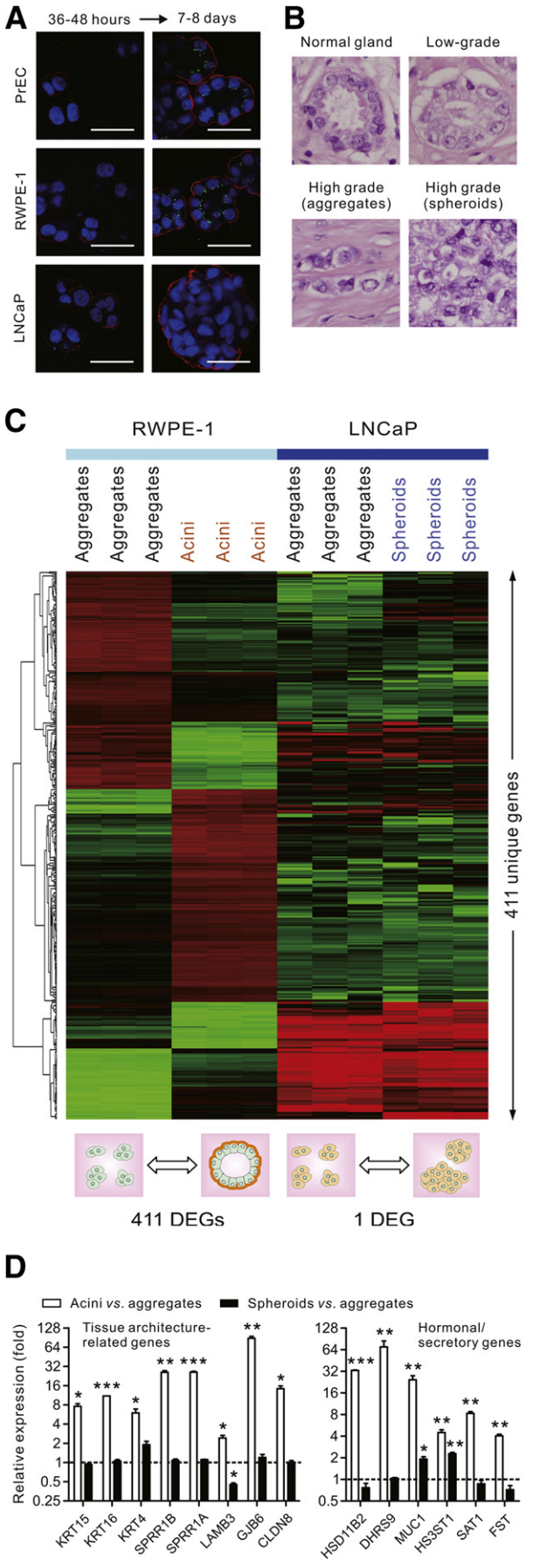


expression patterns that accompanied this morphological program. Given that RWPE-1 cells showed a similar morphological behavior in rBM to primary prostate epithelial cells, we opted to profile the gene expression pattern of this immortalized prostate epithelial cell line compared with the gene expression exhibited by colonies of malignant LNCaP cells. We then conducted comparative transcriptomic analysis to identify genes whose transcript levels varied considerably among all of the samples, with a false-discovery rate of $<0.025$. We identified a list of 411 unique genes (447 probe sets) that showed differential expression during the acinar differentiation of RWPE-1 cells (Figure 1C). As a comparison, we found surprisingly few transcriptional changes associated with the growth of LNCaP tumor spheroids, with only one of the 411 genes exhibiting significant expressional changes. In addition, we found that the transition of RWPE-1 cells from monolayers on rBM-coated plastics to cellular aggregates formed within 3D rBM was not associated with significant transcriptional alterations in these cells (Supplemental Figure S1). These results collectively indicated that the developmental process of prostatic glandular architectures involved distinct transcriptional alterations that were not shared by the unorganized aggregation of malignant cells or the transition among different culture contexts.

Next, to understand, at the functional level, the process of prostatic acinar differentiation, we surveyed the 411 differentially expressed genes for enriched biological processes. Gene ontology functional clustering analysis revealed that the genes up-regulated during prostate acinar morphogenesis were substantially enriched for those related to epithelial and ectodermal differentiation and maintenance of epithelial architectures (Supplemental Figure S2). These included the cytokeratin proteins *KRT15*, *KRT16*, and *KRT4*; the keratinocyte membranous proteins *SPRR1B* and *SPRR1A*; the laminin-5 subunit *LAMB3*; the gap junction proteins *GJB6* and *GJB3*; the tight junction protein *CLDN8*; and the differentiation-associated transcriptional factors *KLF4* and *FOXQ1* (Figure 1D). Complementing this result, functional analysis of these genes by the Ingenuity Pathway Analysis program revealed that they were enriched for biological

**Figure 1** Profiling structural and functional differentiation of prostatic epithelial cells. **A:** Representative confocal images of the prostatic organoids formed by primary prostate epithelial PrECs, RWPE-1 cells, or malignant LNCaP cells in 3D rBM. The structures were immunostained with basal extracellular membrane receptor α6-integrin (red) and the apical marker GM130 (green). Nuclei were counterstained with Hoechst 33342 (blue). Scale bar = 20 μm. **B:** Representative histological sections (H&E) of a normal human prostatic gland and low- or high-grade PCA tissues. Original magnification, ×400. **C:** Hierarchical clustering of 411 differentially expressed genes (DEGs) during prostatic acinar morphogenesis. The heat map depicts high (red) and low (green) relative levels of medium-centered gene expression in log space. **D:** Fold changes in the transcript levels of the genes associated with epithelial differentiation or the hormonal or secretory functions of prostatic glands in RWPE-1 acini or LNCaP spheroids versus cellular aggregates, as measured by quantitative real-time RT-PCR analysis. Data are represented as mean ± SEM ($n = 3$). $^*P < 0.05$, $^{**}P < 0.01$, and $^{***}P < 0.001$.

functions involving cell movement, growth, and development and organ or tissue development (Supplemental Table S1). Notably and more important, further interrogation of these genes identified several factors related to the hormonal and secretory functions of prostatic glands, including steroid and progesterone metabolism (*HSD11B2* and *DHRS9*), mucin or heparin sulfate production (*MUC1* and *HS3ST1*), spermidine/spermine metabolism (*SAT1*), and the gonadal protein (*FST* ); these factors were profoundly up-regulated in RWPE-1 acini compared with cell clusters (Figure 1D). We further demonstrated that these structural and functional genes displayed similar transcriptional changes during the acinar morphogenetic process of primary PrECs (Supplemental Figure S3); however, they were only minimally altered during the growth of LNCaP tumor spheroids (Figure 1D). Taken together, these findings lend strong support to our tissue organization model as a valid way to capture the molecular signals specific to the structural and functional differentiation processes of prostatic glands.

## Acini-Like PCA Linked to Favorable Clinical Prognosis

Prevailing tumor models suggested that cancer was driven by the progressive accumulation of perturbations in genes and pathways that control cell growth and differentiation. In line with this paradigm, we observed that the genes associated with prostatic acinar differentiation were enriched for those functionally related to cancer [163 (39.7%) of 411 genes] (Supplemental Table S1). This finding, together with the biological and prognostic roles of tissue architectural differentiation in human PCA,[5,7] prompted us to posit that this differentiation-associated molecular profile might carry significant prognostic information for PCA. To test this, we interrogated a gene expression microarray data set consisting of 50 patients with localized PCA who underwent radical prostatectomy (the BWH cohort) (Table 1).[10] We determined the degree of resemblance between the patient tumors and prostatic acini by calculating the correlation coefficients ($r_{acinus}$) based on the expression of the 411 acinar morphogenesis–specific genes (Figure 2A). We designated the tumors with higher $r_{acinus}$ acini-like tumors and found that patients with this type of tumor exhibited significantly lower risk for relapse compared with those with lower correlation values by Kaplan-Meier analysis (hazard ratio, 0.078; log-rank test $P = 0.009$) (Figure 2B and Supplemental Table S2). In a multivariate Cox proportional-hazards analysis, the $r_{acinus}$ of the tumors was the only significant predictor of relapse (hazard ratio, 0.173; $P = 0.016$) (Figure 2B and Supplemental Table S3). We repeated the previously described analysis in an independent series of 28 PCA tumors (the SU/KI/JHU cohort) (Table 1)[16] with similar clinical (age and recurrence rate) and pathological (Gleason score, PSA, and stage) features with those tumors in the BWH cohort ($P > 0.05$ by *t*-test or Fisher's exact test). We found that the patients with acini-like tumors fared better than those with lower $r_{acinus}$ in this validation set (hazard ratio, 0.041; log-rank test $P = 0.032$) (Figure 2C and Supplemental Table S2). Multivariate analysis confirmed that $r_{acinus}$ provided independent prognostic information in PCA, whereas the Gleason score was only marginally prognostic in this cohort (Figure 2C and Supplemental Table S3).

After having demonstrated the prognostic value of the gene expression profile–associated prostatic acinar morphogenesis, we next asked if comparison among the molecular characteristics of malignant PCA architectures or microtumors formed in 3D organotypic culture might also provide prognostic information to PCA. To this end, we grew different androgen-sensitive and androgen-insensitive PCA cell lines in 3D rBM and profiled their gene expressions. Surprisingly, none of the gene sets identified by comparing these prostate microtumors had significant correlations with the prognosis of patients with PCA (Supplemental Figure S4). These data suggested that the molecular variations among developed prostate architectures might provide less prognostic information than those associated with the differentiation process of prostatic glandular architectures.

## Identification of Tissue Architecture–Specific Prognostic Markers

The marked prognostic value of a prostatic acinar morphogenesis–associated expression profile in human PCA raised the possibility that this profile might provide an informative basis for identifying markers with strong prognostic value. Thus, we mapped the 411 genes to the tumor transcriptome of the BWH data set and constructed a recurrence score (RS) based on the Cox model to predict the occurrence of tumor relapse. The performance in the prognostic prediction, as assessed by the *C*-index, reached a plateau when a set of 12 genes was selected (Figure 3A). Most of the genes in this set, including sialyltransferase 7B (*ST6GALNAC2*), *ABCG1*, biotinidase (*BTD*), *PDCD4*, *KLF6*, insulin receptor substrate 1 (*IRS1*), zinc finger protein 185 (*ZNF185*), annexin A11 (*ANXA11*), dual-specificity phosphatase 2 (*DUSP2*), Kruppel-like factor 4 (*KLF4*), and desmocollin 2 (*DSC2*), were up-regulated in prostatic acini and were associated with lower risks of disease relapse (Supplemental Table S4). These genes exhibited tissue architecture–dependent modulation of gene expression (Supplemental Figure S5), and many of them might function as candidate tumor suppressors, according to published biological studies.[10,35–40] More important, an RS calculated based on the expression profile of these genes could effectively stratify risk of disease recurrence in independent series of PCA tumors (Figure 3B). By multivariate analyses, this 12-gene model provided strong and independent prognostic information to PCA and markedly enhanced the prognostic accuracy of clinical and pathological variables (Supplemental Tables S5–S7).[10,11,41]

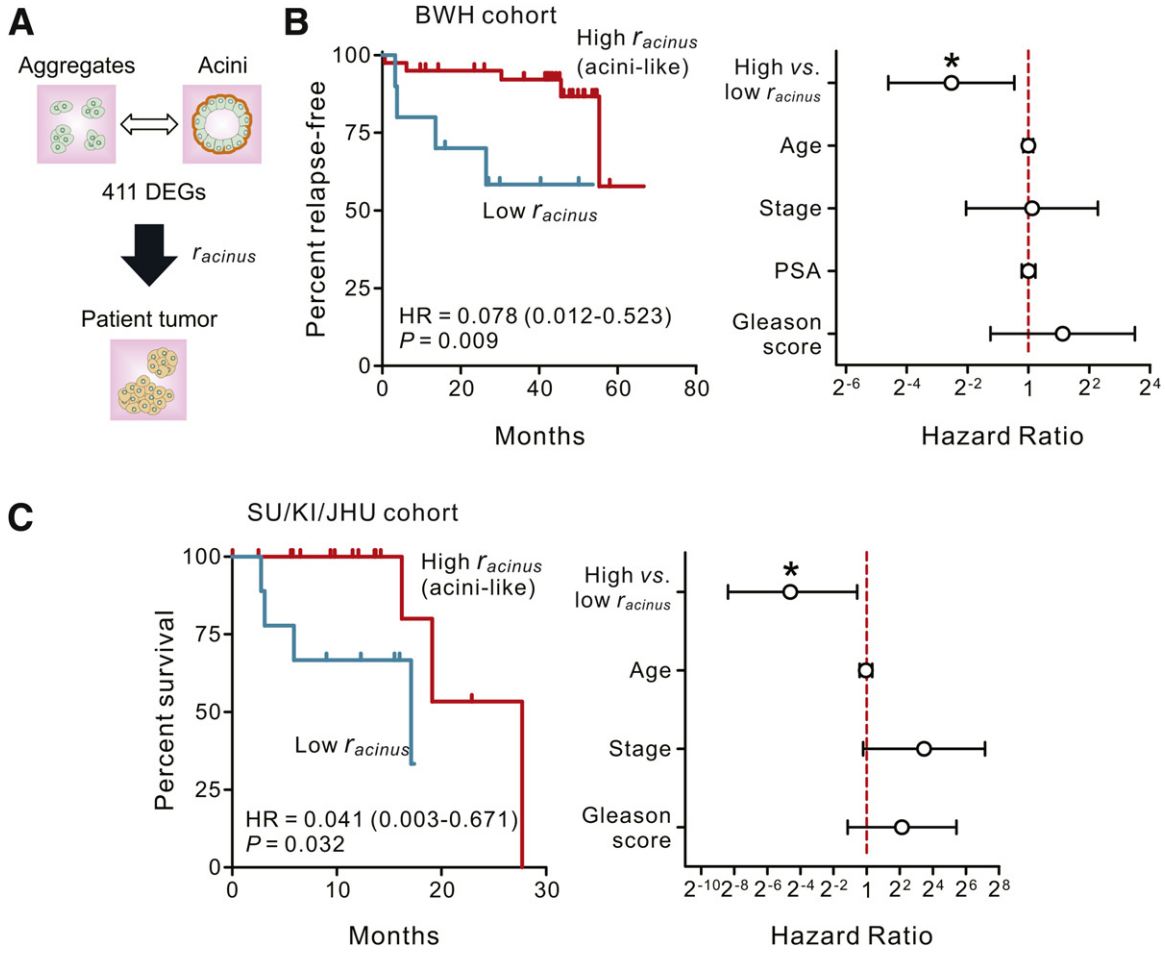


**Figure 2** Acini-like PCA has a reduced risk of postoperative disease relapse. **A:** A schematic representation depicting the derivation of $r_{acinus}$. DEG, differentially expressed gene. **B:** Kaplan-Meier survival curves (**left panel**) comparing relapse-free survival of patients with PCA in the BWH cohort with a high (acini-like) or low $r_{acinus}$ value of their tumors. The *P* value is calculated using the log-rank test. A hazard ratio (HR) plot (**right panel**) (with 95% confidence limits) of disease relapse, according to $r_{acinus}$, age, tumor stage, and PSA or Gleason score in a Cox proportional hazards analysis. **C:** Kaplan-Meier survival curves (**left panel**) comparing relapse-free survival of patients with PCA in the SU/KI/JHU cohort, stratified according to $r_{acinus}$. An HR plot of disease relapse (**right panel**), according to $r_{acinus}$ or clinicopathological criteria in a Cox proportional hazards analysis. $^*P < 0.05$.

Next, seeking to determine whether the prognostic correlation of these genes could be observed at the protein and the tissue levels, we focused on three top-ranked genes with validated antibodies for IHC, including *PDCD4*, *KLF6*, and *ABCG1*. We surveyed their tissue expressions by performing IHC staining of the FFPE tumor tissue sections from a cohort of 61 patients with PCA who underwent radical prostatectomy (the CFMC cohort) (Table 1 and Figure 3C). Indeed, the staining intensities of *PDCD4*, as assessed by the H-score (Supplemental Figure S6), showed strong negative associations with risk of postoperative biochemical recurrence by Kaplan-Meier analysis (log-rank test $P \leq 0.001$) (Figure 3D). We also found that tumors that stained intensely with *KLF6* or *ABCG1* were associated with significantly longer recurrence-free survival compared with those with lower staining intensities (log-rank test $P \leq 0.001$) (Figure 3D). Multivariate analyses showed that the tissue expression level of each of these genes was prognostic, independent of clinical criteria or Gleason score (Supplemental Table S8).

## *PCDC4* and *KLF6* as Regulators and Surrogate Markers of Prostatic Tissue Architectures

Recent studies demonstrated that *KLF6* or *PDCD4* regulated the expression of the cell adhesion molecule, E-cadherin,[36,37] raising a possibility of their potential roles in the maintenance of epithelial tissue architecture. Multiple lines of evidence supported this possibility. First, in human PCA tissues, the staining intensities of *PDCD4* or *KLF6* were inversely correlated with Gleason score ($P < 0.05$) (Figure 4A). Second, we demonstrated that the expression of *PDCD4* or *KLF6* was reciprocally linked to the state of tissue differentiation (Figure 4B). Specifically, the transcript levels of *PDCD4* or *KLF6* increased significantly during the acinar morphogenetic process of prostate epithelial cells. However, structural disruption of prostatic acini by functional inhibition of E-cadherin prevented the increase in their expressions. Moreover, the context-dependent regulation of *PDCD4* or *KLF6* expression was reversible, because

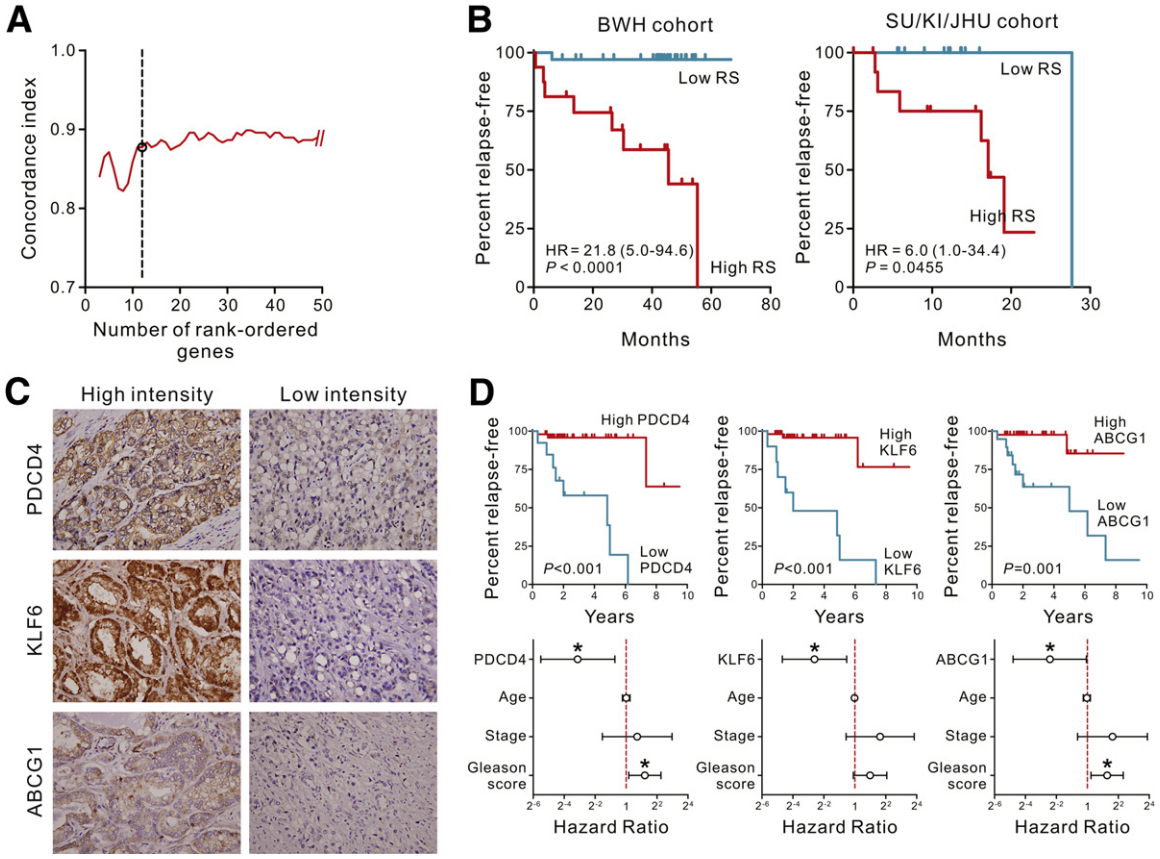


**Figure 3** Identification of tissue architecture–specific prognostic markers of PCA. **A**: Selection of a 12-gene set based on the distribution of the concordance index in the prediction of risk of disease relapse. **B**: Kaplan-Meier survival curves comparing relapse-free survival of patients with PCA in the BWH cohort or the SU/KI/JHU cohort. The patients were stratified into two groups based on the RS, calculated based on the expression profile of the 12-gene set as selected in **A**. The *P* values are calculated using the log-rank test. **C**: Representative immunostaining of *PDCD4*, *KLF6*, and *ABCG1* in PCA tissues. Original magnification, ×400. Tumors with high (**left panels**) or low (**right panels**) staining intensities of the respective markers are shown. **D**: Kaplan-Meier survival curves (**top panels**) comparing recurrence-free survival of patients with PCA in the CFMC cohort, stratified according to the staining intensities of *PDCD4*, *KLF6*, or *ABCG1*. The *P* values are calculated using the log-rank test. Hazard ratio (HR) plots (with 95% confidence limits) of disease relapse (**bottom panels**), according to the staining intensities of *PDCD4*, *KLF6*, or *ABCG1*, or clinicopathological criteria in a Cox proportional hazards analysis. $*P < 0.05$.

the cellular aggregates recovered from prostatic acini had similar expression levels of *PDCD4* or *KLF6* with those measured in the original (ie, primary) cellular aggregates. Third, by using retrovirus-mediated RNAi (Figure 4C), we found that selective down-regulation of the expression of either *PDCD4* or *KLF6* could profoundly cripple the ability of RWPE-1 cells to form polarized prostatic cysts in 3D rBM (Figure 4D).

The critical roles of *PDCD4* and *KLF6* in the regulation of prostatic tissue architectures prompted us to investigate if they could together form a signature that was prognostic of disease recurrence in human PCA. Indeed, an RS calculated based on the staining intensities of *PDCD4*, *KLF6*, and *ABCG1* could stratify the risk of postoperative relapse, with a remarkable accuracy in the CFMC cohort (*C*-index = 0.951) (Figure 5 and Supplemental Table S9), and greatly outperformed a combined clinical model ($P = 0.001$) (Supplemental Table S10). In a multivariate Cox proportional-hazards analysis, the three-gene model–based RS was the only significant prognostic predictor (hazard ratio, 22.591; $P = 0.004$) (Supplemental Table S11). The prognostic prediction could also achieve high accuracy when the transcript abundance levels of these makers were used (*C*-index = 0.939; the BWH cohort) (Figure 5 and Supplemental Tables S10 and S11). To further verify the clinical utility of this three-gene prognostic model, we performed IHC staining of *PDCD4*, *KLF6*, and *ABCG1* in another independent series of 50 PCA tumors (the Mackay Memorial Hospital cohort) (Table 1). Indeed, an RS calculated based on the staining intensities of these genes could stratify patients into prognostic groups (hazard ratio, 9.7; log-rank $P = 0.0009$) (Figure 5 and Supplemental Table S10). We confirmed that the three-gene model–based RS greatly outperformed a combined clinical model ($P < 0.001$) (Supplemental Table S10) and was a strong and independent predictor of postoperative relapse in this validation data set (hazard ratio, 20.234; $P = 0.002$) (Supplemental Table S11). Collectively, the robust prognostic utility of *PDCD4* and *KLF6* and their functional importance in prostate epithelial architectures established them as surrogate markers of tissue

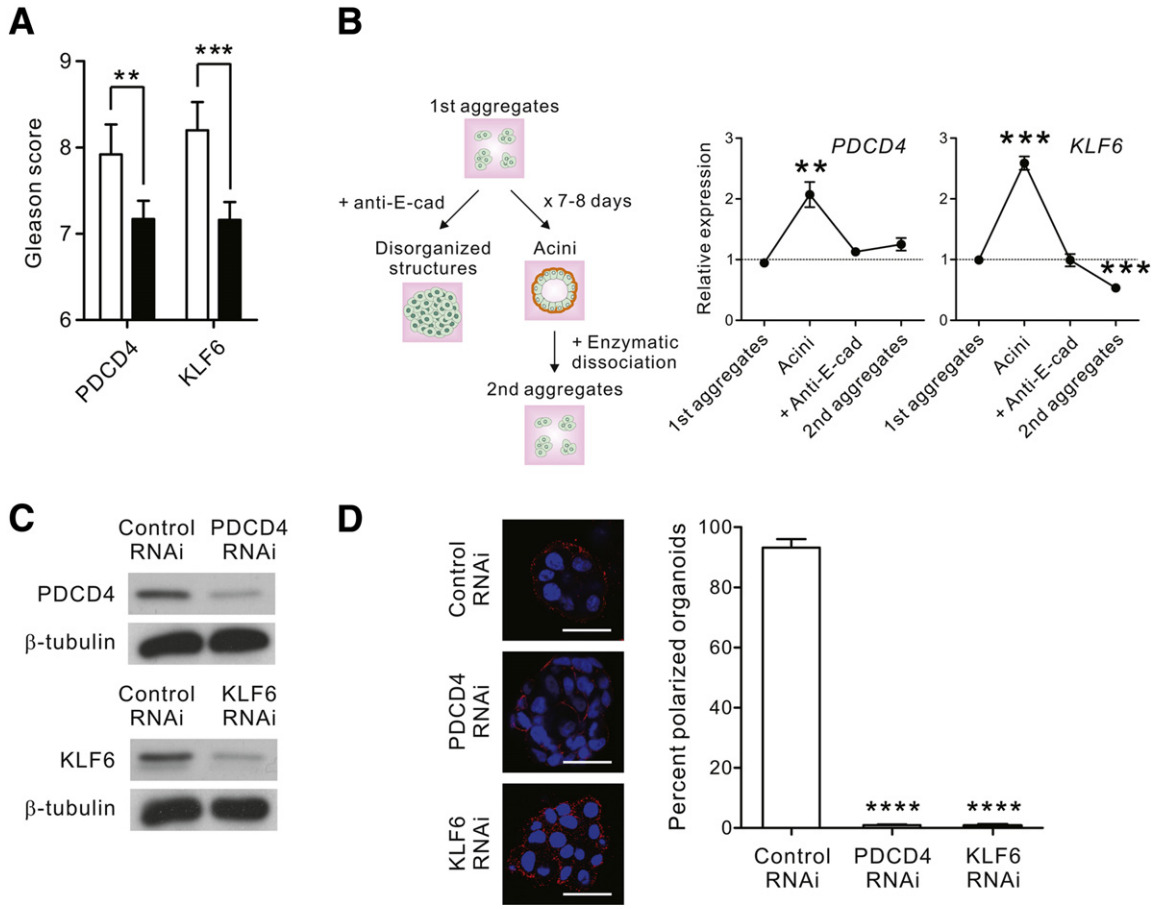


**Figure 4** The roles of *PDCD4* and *KLF6* in prostatic tissue architectures. **A:** Gleason scores of the PCA tumors in the CMFC cohort with high (black bars) or low (white bars) staining intensities of *PDCD4* or *KLF6*. Data are represented as mean ± SEM. $*P < 0.1$, $**P < 0.05$. **B:** Schematic representation of the experimental protocol for growing different prostatic tissue architectures. RWPE-1 cells were grown in 3D rBM as primary cellular aggregates (first aggregates) or acini (**left panel**). The formation of acinar architecture was abrogated by incorporating a function-blocking antibody of E-cadherin (anti—E-cad) in the matrices. Alternatively, the cells were recovered from differentiated acini by enzymatic digestion and re-embedded in 3D rBM to allow for the growth of secondary cellular aggregates (second aggregates). The transcript abundance levels of PDCD4 and KLF6 in different prostatic tissue architectures, as measured by quantitative real-time RT-PCR analysis (**right panel**). Data are represented as mean ± SEM ($n = 3$). $**P < 0.05$, $***P < 0.01$ versus first aggregates. **C:** Immunoblotting showing the effect of RNAi-mediated knockdown of *PDCD4* or *KLF6* in RWPE-1 cells. β-Tubulin was included as a loading control. **D:** Representative confocal images of the prostatic organoids formed by *PDCD4*- or *KLF6*-deficient RWPE-1 cells or the control RNAi cells in 3D rBM (**left panel**). The structures were immunostained with basal extracellular membrane receptor α6-integrin (red). Nuclei were counterstained with Hoechst 33342 (blue). Scale bar = 20 μm. Percentage of polarized organoids, as quantified by visual examination and counting under a fluorescence microscope (**right panel**). Data are represented as mean ± SEM ($n = 25$). $****P < 0.001$ versus control.

differentiation that were linked to clinical outcomes of patients with PCA.

## Discussion

Molecular characterization of malignant tumors can aid disease classification and the prognostic prediction of the patients.[14,42,43] Herein, we summarize our findings, which exploited the experimental merits of a physiologically relevant model of tissue differentiation, to identify a molecular signature that reflects prostate tumors with a better prognosis. Our signature, which was informed by the gene expression profile of differentiated prostate epithelial acini, specifically identifies prostate tumors with a more differentiated phenotype. We used our architecture-related signature to identify a subset of human PCA that exhibits a favorable outcome. This novel and biology-informed molecular classification system considerably outperforms clinical and pathological criteria and improves prognostic prediction in several independent cohorts of patients with PCA. Thus, our results offer critical insight toward the functional link between tissue architectures and PCA in human tissue and, to our knowledge, provide the first ever set of biologically relevant molecular markers that have potential clinical utility.

One of the major challenges in the care of patients with early-stage PCA is the ability to identify those patients who are at risk for early relapse after surgery. Clinical and pathological criteria fail to provide an accurate prediction of tumor relapse. Accordingly, there have been numerous attempts to improve prognostic prediction by constructing accurate profiles of the molecular characterizations of the excised prostate tumors, with varying success.[10,11] For instance, correlating the tumor transcriptome data with clinical outcome data in a relatively small cohort ($n = 21$)

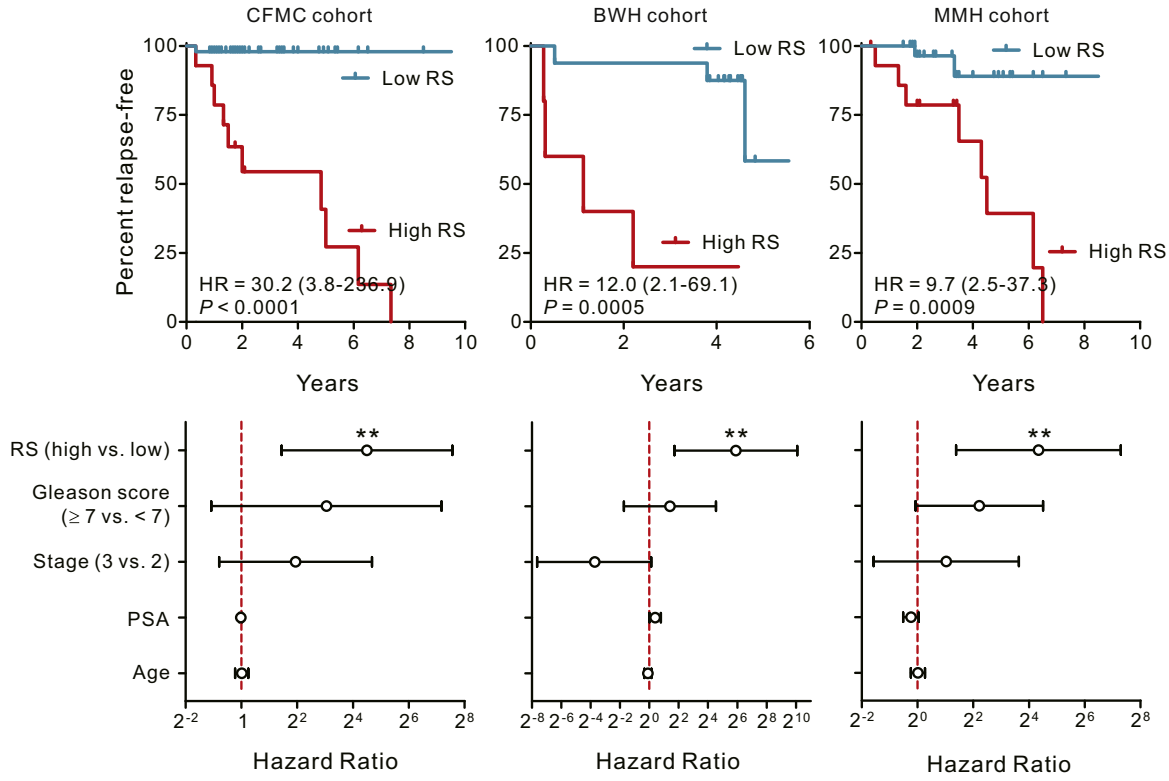


**Figure 5** *PDCD4*, *KLF6*, and *ABCG1* form a three-gene prognostic signature in human PCA. **Top panels**, Kaplan-Meier survival curves comparing relapse-free survival of patients in different series of PCA tumors with a high and low RS calculated based on the staining intensities (for the CFMC and the Mackay Memorial Hospital cohorts) or the transcript abundance levels (for the BWH cohort) of *PDCD4*, *KLF6*, and *ABCG1*. HR, hazard ratio. The *P* value is calculated using the log-rank test. **Bottom panels**, HR plots (with 95% confidence limits) of disease relapse according to the RS or clinicopathological criteria in a Cox proportional hazards analysis. $^{**}P < 0.01$.

of patients with PCA, Singh et al[10] demonstrated that the expression pattern of a set of five gene markers in the excised primary tumors could be used to accurately predict the clinical behaviors of PCA. In another example, comparative transcriptomic analysis on recurrent or nonrecurrent human PCA and metastatic xenografted tumors in mice resulted in the identification of several PCA gene signatures that possessed validated prognostic values.[11] More recently, Malhotra et al[41] developed a proliferative index of PCA based on the IHC staining patterns of three proliferation-related gene markers, including *MKI67*, *TOP2A*, and *E2F1*, which improved prognostic prediction in a cohort of 139 patients with PCA. However, unfortunately, these molecular markers have yet to be adopted in clinical practice, in part because of the pressing need for additional large-scale performance testing, but also possibly because of their lack of mechanistic insight and/or biological demonstrated relevance to prostate tissue transformation. In the present study, we identified the first biologically tractable prognostic signature of PCA, which, in addition, presents a plausible mechanism linked to tissue-specific differentiation and adhesion-dependent tissue architecture. Our signature supplements the Gleason score and can function as a viable prognostic predictor of patients with PCA. Moreover, our signature can provide a much-needed means to molecularly define differentiated PCA. Presumably, this knowledge-based classification system may improve the prognostic prediction of PCA and permit the development of rational personalized therapeutic strategies to treat PCA.

By using a 3D morphogenesis assay, we demonstrated that the expression of prostatic acinar morphogenesis-associated genes is tightly regulated by tissue organization. Interestingly, some of these genes passively respond to tissue architecture cues and are reciprocally linked to the assembly of tissue organization. Thus, we found that down-regulating *PDCD4* or *KLF6* in prostate epithelial cells disrupted their acinar morphogenesis. Such a functional role for these differentiation-associated genes with PCA behavior may explain their significant correlation to PCA Gleason score and the clinical prognosis of patients with PCA. For instance, the gene *PDCD4* encodes a candidate tumor suppressor that targets translation initiation[44] and reduces the growth of PCA cells through down-regulation of Y-box–binding protein-1 expression.[45] The gene *KLF6* encodes a zinc finger transcription factor that can up-regulate p21 and is mutated in 70% of human PCA and lost in high-grade tumors.[35,46] Interestingly and more important, both *KLF6* and *PDCD4* induce expression of the cell adhesion molecule, E-cadherin,[36,37] providing a mechanistic explanation of their roles in tissue architecture. Other constituent genes in the acinar morphogenesis–associated 12-gene signature, such as *KLF4* and *IRS1*, may also regulate prostate epithelial architecture by reducing cell migration/invasion or increasing extracellular membrane–dependent adhesion in prostate cancer cells.[38,40] On the other hand, there is abundant

evidence that supports a prognostic role of the other genes in the signature, although the mechanisms underlying their pathogenetic roles in PCA are less clear. For instance, the only secreted protein in the signature, biotinidase (*BTD*), was identified as a serum biomarker for Gleason score prediction in PCA.[47] The gene *DUSP2* encodes a dual-specificity phosphatase that is a negative regulator of mitogen-activated protein kinases and is markedly reduced in human PCA tissues.[39] Finally, although no report has directly linked the top-ranked gene in the signature, *ST6GALNAC2*, to the prognosis of PCA, another sialyltransferase, sialyltransferase 1, is the major gene marker in the five-gene signature identified by Singh et al.[10]

The clinical utility of biomarkers can be greatly enhanced if they can be detected in FFPE tissue sections that are routinely available for pathological examination. Because we noted that most of the gene markers in our 12-gene signature exhibit significant prognostic value in PCA, we believe that it may be feasible to identify a specific combination of these markers for clinical prediction of patient prognosis. In particular, our data indicate one particular combination, consisting of *PDCD4*, *KLF6*, and *ABCG1*, and we showed that this combination of markers can be readily detected by IHC and can provide strong and robust prognostic information for PCA. We further demonstrated that mRNA levels of these markers can provide equally accurate prognostic prediction in patients with PCA, thereby providing an alternate strategy to screen for prognostic markers in PCA patient tissue. By using either IHC or RNA screening approaches, it is feasible to conduct a large-scale validation of our prognostic signature using frozen tumor materials (for mRNA) or FFPE tissues (for IHC staining) collected from either prospective or retrospective clinical trials. Furthermore, aside from this three-gene combination, our preliminary analysis also showed that any two of these genes (eg, *PDCD4* versus *KLF6* or *PDCD4* versus *ABCG1*) function as a robust prognostic predictor with high accuracy in independent patient cohorts (*C*-index up to 0.915; data not shown). Such findings imply that other clinical useful combinations of these architecture-specific markers may exist and merit further evaluation.

In summary, our results illustrate that interrogation of the transcriptional program associated with prostate acinar differentiation is able to be exploited to generate a strong and robust prognostic predictor for human PCA. The architecture-related gene signature is strong and independent of clinicopathological criteria, reinforcing the idea that biomarkers constructed based on crucial tumor biological characteristics could significantly improve disease classification and outcome prediction. Whether the same approach could be applied to the identification of prognostic markers in more advanced PCA or other types of glandular cancers awaits further investigation.

## Supplemental Data

Supplemental material for this article can be found at *http://dx.doi.org/10.1016/j.ajpath.2012.10.024*.

## References


1. Bill-Axelson A, Holmberg L, Ruutu M, Haggman M, Andersson SO, Bratell S, Spangberg A, Busch C, Nordling S, Garmo H, Palmgren J, Adami HO, Norlen BJ, Johansson JE: Radical prostatectomy versus watchful waiting in early prostate cancer. N Engl J Med 2005, 352: 1977–1984
2. Pound CR, Partin AW, Eisenberger MA, Chan DW, Pearson JD, Walsh PC: Natural history of progression after PSA elevation following radical prostatectomy. JAMA 1999, 281:1591–1597
3. Gorlov IP, Byun J, Gorlova OY, Aparicio AM, Efstathiou E, Logothetis CJ: Candidate pathways and genes for prostate cancer: a meta-analysis of gene expression data. BMC Med Genomics 2009, 2:48
4. Gorlov IP, Sircar K, Zhao H, Maity SN, Navone NM, Gorlova OY, Troncoso P, Pettaway CA, Byun JY, Logothetis CJ: Prioritizing genes associated with prostate cancer development. BMC Cancer 2010, 10:599
5. Zhang X, Fournier MV, Ware JL, Bissell MJ, Yacoub A, Zehner ZE: Inhibition of vimentin or beta1 integrin reverts morphology of prostate tumor cells grown in laminin-rich extracellular matrix gels and reduces tumor growth in vivo. Mol Cancer Ther 2009, 8:499–508
6. True L, Coleman I, Hawley S, Huang CY, Gifford D, Coleman R, Beer TM, Gelmann E, Datta M, Mostaghel E, Knudsen B, Lange P, Vessella R, Lin D, Hood L, Nelson PS: A molecular correlate to the Gleason grading system for prostate adenocarcinoma. Proc Natl Acad Sci U S A 2006, 103:10991–10996
7. Gleason DF: Histologic grading of prostate cancer: a perspective. Hum Pathol 1992, 23:273–279
8. Stamey TA, McNeal JE, Yemoto CM, Sigal BM, Johnstone IM: Biological determinants of cancer progression in men with prostate cancer. JAMA 1999, 281:1395–1400
9. Albertsen PC, Fryback DG, Storer BE, Kolon TF, Fine J: Long-term survival among men with conservatively treated localized prostate cancer. JAMA 1995, 274:626–631
10. Singh D, Febbo PG, Ross K, Jackson DG, Manola J, Ladd C, Tamayo P, Renshaw AA, D'Amico AV, Richie JP, Lander ES, Loda M, Kantoff PW, Golub TR, Sellers WR: Gene expression correlates of clinical prostate cancer behavior. Cancer Cell 2002, 1: 203–209
11. Glinsky GV, Glinskii AB, Stephenson AJ, Hoffman RM, Gerald WL: Gene expression profiling predicts clinical outcome of prostate cancer. J Clin Invest 2004, 113:913–923
12. Stratford JK, Bentrem DJ, Anderson JM, Fan C, Volmar KA, Marron JS, Routh ED, Caskey LS, Samuel JC, Der CJ, Thorne LB, Calvo BF, Kim HJ, Talamonti MS, Iacobuzio-Donahue CA, Hollingsworth MA, Perou CM, Yeh JJ: A six-gene signature predicts survival of patients with localized pancreatic ductal adenocarcinoma. PLoS Med 2010, 7:e1000307
13. van't Veer LJ, Dai H, van de Vijver MJ, He YD, Hart AA, Mao M, Peterse HL, van der Kooy K, Marton MJ, Witteveen AT, Schreiber GJ, Kerkhoven RM, Roberts C, Linsley PS, Bernards R, Friend SH: Gene expression profiling predicts clinical outcome of breast cancer. Nature 2002, 415:530–536
14. van de Vijver MJ, He YD, van't Veer LJ, Dai H, Hart AA, Voskuil DW, Schreiber GJ, Peterse JL, Roberts C, Marton MJ, Parrish M, Atsma D, Witteveen A, Glas A, Delahaye L, van der Velde T, Bartelink H, Rodenhuis S, Rutgers ET, Friend SH, Bernards R: A gene-expression signature as a predictor of survival in breast cancer. N Engl J Med 2002, 347:1999–2009
15. Henshall SM, Afar DE, Hiller J, Horvath LG, Quinn DI, Rasiah KK, Gish K, Willhite D, Kench JG, Gardiner-Garden M, Stricker PD, Scher HI, Grygiel JJ, Agus DB, Mack DH, Sutherland RL: Survival analysis of genome-wide gene expression profiles of prostate cancers identifies new prognostic targets of disease relapse. Cancer Res 2003, 63:4196–4203

16. Lapointe J, Li C, Higgins JP, van de Rijn M, Bair E, Montgomery K, Ferrari M, Egevad L, Rayford W, Bergerheim U, Ekman P, DeMarzo AM, Tibshirani R, Botstein D, Brown PO, Brooks JD, Pollack JR: Gene expression profiling identifies clinically relevant subtypes of prostate cancer. Proc Natl Acad Sci U S A 2004, 101: 811–816
17. Bibikova M, Chudin E, Arsanjani A, Zhou L, Garcia EW, Modder J, Kostelec M, Barker D, Downs T, Fan JB, Wang-Rodriguez J: Expression signatures that correlated with Gleason score and relapse in prostate cancer. Genomics 2007, 89:666–672
18. Sotiriou C, Wirapati P, Loi S, Harris A, Fox S, Smeds J, Nordgren H, Farmer P, Praz V, Haibe-Kains B, Desmedt C, Larsimont D, Cardoso F, Peterse H, Nuyten D, Buyse M, Van de Vijver MJ, Bergh J, Piccart M, Delorenzi M: Gene expression profiling in breast cancer: understanding the molecular basis of histologic grade to improve prognosis. J Natl Cancer Inst 2006, 98:262–272
19. Chang HY, Sneddon JB, Alizadeh AA, Sood R, West RB, Montgomery K, Chi JT, van de Rijn M, Botstein D, Brown PO: Gene expression signature of fibroblast serum response predicts human cancer progression: similarities between tumors and wounds. PLoS Biol 2004, 2:E7
20. Fournier MV, Martin KJ, Kenny PA, Xhaja K, Bosch I, Yaswen P, Bissell MJ: Gene expression signature in organized and growth-arrested mammary acini predicts good outcome in breast cancer. Cancer Res 2006, 66:7095–7102
21. Liu R, Wang X, Chen GY, Dalerba P, Gurney A, Hoey T, Sherlock G, Lewicki J, Shedden K, Clarke MF: The prognostic role of a gene signature from tumorigenic breast-cancer cells. N Engl J Med 2007, 356:217–226
22. Bello D, Webber MM, Kleinman HK, Wartinger DD, Rhim JS: Androgen responsive adult human prostatic epithelial cell lines immortalized by human papillomavirus 18. Carcinogenesis 1997, 18:1215–1223
23. Weaver VM, Petersen OW, Wang F, Larabell CA, Briand P, Damsky C, Bissell MJ: Reversion of the malignant phenotype of human breast cells in three-dimensional culture and in vivo by integrin blocking antibodies. J Cell Biol 1997, 137:231–245
24. Lee GY, Kenny PA, Lee EH, Bissell MJ: Three-dimensional culture models of normal and malignant breast epithelial cells. Nat Methods 2007, 4:359–365
25. Wang Y, Klijn JG, Zhang Y, Sieuwerts AM, Look MP, Yang F, Talantov D, Timmermans M, Meijer-van Gelder ME, Yu J, Jatkoe T, Berns EM, Atkins D, Foekens JA: Gene-expression profiles to predict distant metastasis of lymph-node-negative primary breast cancer. Lancet 2005, 365:671–679
26. Pencina MJ, D'Agostino RB: Overall C as a measure of discrimination in survival analysis: model specific population value and confidence interval estimation. Stat Med 2004, 23:2109–2123
27. Narla G, DiFeo A, Yao S, Banno A, Hod E, Reeves HL, Qiao RF, Camacho-Vanegas O, Levine A, Kirschenbaum A, Chan AM, Friedman SL, Martignetti JA: Targeted inhibition of the KLF6 splice variant, KLF6 SV1, suppresses prostate cancer cell growth and spread. Cancer Res 2005, 65:5761–5768
28. Stephenson AJ, Kattan MW, Eastham JA, Dotan ZA, Bianco FJ Jr, Lilja H, Scardino PT: Defining biochemical recurrence of prostate cancer after radical prostatectomy: a proposal for a standardized definition. J Clin Oncol 2006, 24:3973–3978
29. Budwit-Novotny DA, McCarty KS, Cox EB, Soper JT, Mutch DG, Creasman WT, Flowers JL, McCarty KS Jr: Immunohistochemical analyses of estrogen receptor in endometrial adenocarcinoma using a monoclonal antibody. Cancer Res 1986, 46:5419–5425
30. Pepe MS: The Statistical Evaluation of Medical Tests for Classification and Prediction. New York, Oxford University Press, 2003
31. Yamada KM, Cukierman E: Modeling tissue morphogenesis and cancer in 3D. Cell 2007, 130:601–610
32. Bissell MJ, Rizki A, Mian IS: Tissue architecture: the ultimate regulator of breast epithelial function. Curr Opin Cell Biol 2003, 15: 753–762
33. Debnath J, Brugge JS: Modelling glandular epithelial cancers in three-dimensional cultures. Nat Rev Cancer 2005, 5:675–688
34. Webber MM, Bello D, Kleinman HK, Hoffman MP: Acinar differentiation by non-malignant immortalized human prostatic epithelial cells and its loss by malignant cells. Carcinogenesis 1997, 18: 1225–1231
35. Narla G, Heath KE, Reeves HL, Li D, Giono LE, Kimmelman AC, Glucksman MJ, Narla J, Eng FJ, Chan AM, Ferrari AC, Martignetti JA, Friedman SL: KLF6, a candidate tumor suppressor gene mutated in prostate cancer. Science 2001, 294:2563–2566
36. Wang Q, Sun ZX, Allgayer H, Yang HS: Downregulation of E-cadherin is an essential event in activating beta-catenin/Tcf-dependent transcription and expression of its target genes in Pdcd4 knockdown cells. Oncogene 2010, 29:128–138
37. DiFeo A, Narla G, Camacho-Vanegas O, Nishio H, Rose SL, Buller RE, Friedman SL, Walsh MJ, Martignetti JA: E-cadherin is a novel transcriptional target of the KLF6 tumor suppressor. Oncogene 2006, 25:6026–6031
38. Wang J, Place RF, Huang V, Wang X, Noonan EJ, Magyar CE, Huang J, Li LC: Prognostic value and function of KLF4 in prostate cancer: RNAa and vector-mediated overexpression identify KLF4 as an inhibitor of tumor cell growth and migration. Cancer Res 2010, 70: 10182–10191
39. Lin SC, Chien CW, Lee JC, Yeh YC, Hsu KF, Lai YY, Tsai SJ: Suppression of dual-specificity phosphatase-2 by hypoxia increases chemoresistance and malignancy in human cancer cells. J Clin Invest 2011, 121:1905–1916
40. Reiss K, Wang JY, Romano G, Tu X, Peruzzi F, Baserga R: Mechanisms of regulation of cell adhesion and motility by insulin receptor substrate-1 in prostate cancer cells. Oncogene 2001, 20:490–500
41. Malhotra S, Lapointe J, Salari K, Higgins JP, Ferrari M, Montgomery K, van de Rijn M, Brooks JD, Pollack JR: A tri-marker proliferation index predicts biochemical recurrence after surgery for prostate cancer. PLoS One 2011, 6:e20293
42. Sorlie T, Tibshirani R, Parker J, Hastie T, Marron JS, Nobel A, Deng S, Johnsen H, Pesich R, Geisler S, Demeter J, Perou CM, Lonning PE, Brown PO, Borresen-Dale AL, Botstein D: Repeated observation of breast tumor subtypes in independent gene expression data sets. Proc Natl Acad Sci U S A 2003, 100:8418–8423
43. Andre F, Pusztai L: Molecular classification of breast cancer: implications for selection of adjuvant chemotherapy. Nat Clin Pract Oncol 2006, 3:621–632
44. LaRonde-LeBlanc N, Santhanam AN, Baker AR, Wlodawer A, Colburn NH: Structural basis for inhibition of translation by the tumor suppressor Pdcd4. Mol Cell Biol 2007, 27:147–156
45. Shiota M, Izumi H, Tanimoto A, Takahashi M, Miyamoto N, Kashiwagi E, Kidani A, Hirano G, Masubuchi D, Fukunaka Y, Yasuniwa Y, Naito S, Nishizawa S, Sasaguri Y, Kohno K: Programmed cell death protein 4 down-regulates Y-box binding protein-1 expression via a direct interaction with Twist1 to suppress cancer cell growth. Cancer Res 2009, 69:3148–3156
46. Chen C, Hyytinen ER, Sun X, Helin HJ, Koivisto PA, Frierson HF Jr, Vessella RL, Dong JT: Deletion, mutation, and loss of expression of KLF6 in human prostate cancer. Am J Pathol 2003, 162:1349–1354
47. Cima I, Schiess R, Wild P, Kaelin M, Schuffler P, Lange V, Picotti P, Ossola R, Templeton A, Schubert O, Fuchs T, Leippold T, Wyler S, Zehetner J, Jochum W, Buhmann J, Cerny T, Moch H, Gillessen S, Aebersold R, Krek W: Cancer genetics-guided discovery of serum biomarker signatures for diagnosis and prognosis of prostate cancer. Proc Natl Acad Sci U S A 2011, 108:3342–3347